# Stagnating Turbulent Flows

W. C. Strahle,* R. K. Sigman,† and W. L. Meyer‡
*Georgia Institute of Technology, Atlanta, Georgia*

**An extension of the Lam-Bremhorst two-equation turbulence model to variable-density flows is described, and the method is applied to two-dimensional, planar stagnation-point flows. In the course of this extension, it is found necessary to develop a transport equation for temperature (density) fluctuations. The method is believed to correct past deficiencies in the near-wall behavior of the turbulent field. While the method appears to work for the inner viscous layer, it presents a formidable numerical problem in the solution of a two-point boundary-value problem because of extreme sensitivity of the solution to the boundary values, uncharacteristic of more usual stagnation-point problems. Comparison with stagnation-point heat-transfer data shows excellent agreement of theory and experiment at sufficiently low laminar Reynolds number. At high Reynolds number, an effect of the stagnation process in the nonviscous zone outside the boundary layer predicts an excessive effect of body size on the results, although the agreement is still satisfactory.**

## Nomenclature

$A, A_{C1}, A_t$ = constants in Eqs. (3) and (6)
$c$ = length scale for nondimensionalization
$c_p$ = specific heat at constant pressure
$D$ = cylinder diameter
$E$ = dimensionless dissipation rate, $c/(-V_\infty)^3$
$f$ = $\eta$-dependent function of the stream function
$f_1, f_2, f_\mu$ = functions in Eqs. (3), (4), and (6)
$g$ = dimensionless Favre-averaged temperature
$h$ = $T''/T_\infty$
$K, k$ = dimensionless and Favre-averaged turbulent kinetic energy, respectively
$L_f$ = integral length scale of turbulence
$M$ = turbulence grid mesh size
$p$ = pressure
$P$ = $p/p_\infty$
$p_r$ = molecular Prandtl number
$q$ = $\overline{\rho T''^2}\rho_\infty$
$R$ = dimensionless density, $\rho/\rho_\infty$
$Re_D$ = Reynolds number based on cylinder diameter, $\rho_\infty D(-V_\infty)/\mu_\infty$
$R_k$ = turbulent Reynolds number, $\rho k^{\frac{1}{2}}\eta/\mu$
$R_\ell$ = laminar Reynolds number, $\rho_\infty(-V_\infty)c/\mu_\infty$
$R_t$ = turbulent Reynolds number, $\rho k^2/\epsilon\mu$
$R_T$ = turbulent Reynolds number, $\rho_\infty c(-V_\infty)/\mu_T$
$T$ = temperature
$u_i$ = dimensionless velocity in $i$th coordinate direction, $U_i/(-V_\infty)$
$U_i$ = velocity in $i$th coordinate direction
$u'_\infty$ = relative turbulent intensity in the freestream of axial component of velocity in Ref. 2
$x_i$ = dimensional or dimensionless coordinate in $i$th direction
$y$ = dimensionless coordinate perpendicular to wall
$\gamma$ = inviscid gradient of the parallel velocity component at the stagnation point $*a/(-V_\infty)$
$\epsilon$ = Favre-averaged dissipation rate
$\eta$ = normalized stretched boundary-layer coordinate
$\lambda$ = molecular thermal conductivity
$\mu, \mu_T$ = molecular and turbulent viscosity, respectively
$\sigma_\epsilon$ = constant in dissipation rate equation
$\xi$ = $x$
$\rho$ = density
$\sigma_T$ = turbulent Prandtl number
$\tau_{ij}$ = molecular viscous stress tensor
$\psi$ = stream function

*Subscripts*

0 = turbulence specification station
$\infty$ = freestream values
$s$ = edge of viscous layer

*Superscripts*

$(\bar{\ })$ = time average
$(\ )'$ = differentiation
$(\tilde{\ })$ = Favre average
$(\ )''$ = Favre fluctuation

## Introduction

STAGNATION-POINT heat transfer, when the approach flow contains turbulence, is an important technical issue in several applications. In chemical engineering, typical applications include heat transfer to boiler tubes and in catalyst beds. In aerospace engineering, the impact of a combustor discharge on the nozzle guide vanes in a gas turbine is a typical application as is the flow near a reattachment point behind a flame stabilization step in a ramjet combustor. Analytically, stagnation-point solutions often provide a start for downstream boundary-layer calculations and provide a good estimate for the maximum heat transfer expected in a given situation.

There have been many theoretical expositions of stagnation-point flows with embedded freestream turbulence, Refs. 1–5 among them. However, except for the work by Traci and Wilcox,[4] these expositions have been based on a zeroth-order closure of the turbulence equations with an eddy-viscosity model that cannot behave properly near the wall. In Ref. 4, a two-equation model was used for the turbulence but, again, the model does not behave properly near the wall, which demands that the dissipation rate is finite but that the turbulent kinetic energy rises as the second power of distance from the wall.[6] In the case of variable-density flows, none of the above-mentioned expositions take account of the density (temperature) fluctuations, so that no effective account is

Presented as Paper 86-0437 at the AIAA 24th Aerospace Sciences Meeting, Reno, NV, Jan. 6–9, 1986; received Feb. 3, 1986; revision received Nov. 20, 1986. 

*Regents' Professor of Aerospace Engineering. Fellow AIAA.
†Senior Research Engineer. Member AIAA.
‡Research Engineer. Member AIAA.

taken of the difference between mass-weighted (Favre) or ordinary (Reynolds) time averages of flowfield quantities.

As apparently first pointed out by Jones and Launder,[7] there is always a problem with usual two-equation models of turbulence near a wall, even if a low Reynolds number model is adopted that retains a molecular viscosity effect. Near-wall effects have been investigated by many workers,[6–11] and "fixes" have been made to the turbulence equations in the form of added terms or changed empirical constants or postulated empirical functions multiplying more conventional terms. In this paper, the Lam-Bremhorst[6] two-equation model of turbulence is chosen for extension to the variable-density case. It is a model that changes some "constants" to functions but does not add terms or change the physical meaning of terms in the turbulence equations. This model is chosen purely from the authors' preference for it over other possible approaches. It has the virtues of 1) proper behavior of turbulence quantities near the wall and 2) experimental test against an incompressible pipe flow.

This paper has three purposes. The first is to determine whether the formulation of Ref. 6 can be carried over to the variable-density case without theoretical or numerical difficulty. Second, the theory will be compared with heat-transfer data to test its accuracy. Third, a theoretical formalism will be developed to account for the effect of temperature fluctuations in the approach flow to the stagnation point, which is an effect never before treated.

## Analysis

### Configuration and Outer Flow

Consider the two-dimensional, planar stagnation-point flow of Fig. 1. In incompressible flow, it is well known that an exact solution of the Navier-Stokes equations exists for such a flow. However, a parameter in the solution is the gradient along the surface of the velocity parallel to the surface at the infinity of the viscous layer. This is unknown for an actual flow unless an outer solution is known for the body of interest. This renders the stagnation-point solution useful only for viscous flows that have a thin viscous layer compared to a characteristic dimension of the body, say, the nose radius of curvature. Consequently, a high laminar Reynolds number is required.

In the problem at hand, the approach flow is considered to be a turbulent one, which may contain velocity as well as temperature fluctuations, but a flow with a low Mach number so that compressibility effects are absent. The viscous layer adjacent to the body is expected to be modified (i.e., thickened) by the turbulence and, in order that the viscous zone may be thin compared to the body nose dimension, the turbulence Reynolds number must also be large.

The fluid is assumed to be a perfect gas with constant specific heats. Since it will be found that the static pressure is fairly constant throughout the viscous zone, a usual boundary-layer approximation will be made that $\rho\mu = \rho_\infty \mu_\infty = \text{const.}$

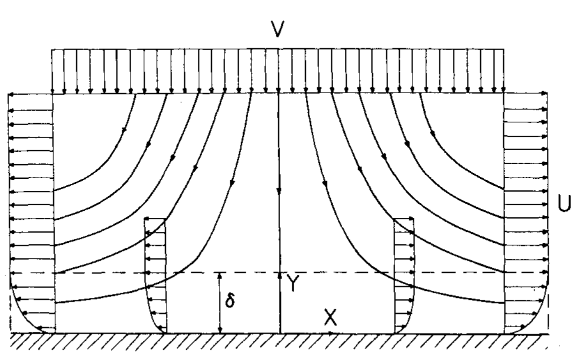


**Fig. 1 Stagnation-point flow configuration.**

Traci and Wilcox[4] appear to be the first to account analytically for the fact that the approach flow toward the stagnation point is actually a three-layer problem. First, there is the flow far from the body but after the last turbulence generation point (say, a grid). In this region, convection of the turbulence is balanced only by dissipation, and the turbulence level decays. In the second region, the flow is starting to stagnate, a mean rate of strain is developed, and turbulence production starts to occur. In Ref. 4, it was presumed that the production, dissipation, and diffusion came into play to balance the convective transport. Here, however, the turbulence Reynolds number has been presumed large so that diffusion is absent. A recent theory of this basically inviscid stagnation process has been constructed using the $k$-$\epsilon$ turbulence model.[12] An exact solution was found to link the "freestream" flow to the edge of the body viscous layer and to form the boundary condition for the outer edge of the viscous layer. This condition is that production balances dissipation at the edge. The linking condition from the viscous edge to the freestream is discussed below.

The production of turbulence during the inviscid part of the deceleration process has experimental support.[13,14] It will be shown to have a large effect on the results.

At this point, it may be helpful to point out that there are several values of the Reynolds number to appear, and the reader may wish to consult the Nomenclature to avoid confusion. In particular, there is a distinction between the following Reynolds numbers, depending on turbulent or mean velocities, molecular or turbulent viscosities, and physical dimension or distance scales:

$$R_\ell, R_T, R_k, R_t, Re_D$$

### Turbulence Model

Consider that quantities are made dimensionless by the freestream values of velocity, density, temperature, and a characteristic dimension $c$, which will be defined later and which will be proportional to the nose radius of curvature. The turbulence model chosen is a modified version of the Lam-Bremhorst two-equation $k$-$\epsilon$ model.[6] It is modified first by presuming it may be carried over from its originally introduced constant density form to a mixed form suggested by Jones.[15] That is, mean quantities other than the density appear as Favre-averaged quantities, the mean density appears as an ordinary time mean, and all fluctuating quantities appear as Favre fluctuations. In this case, the equations for (dimensionless) turbulent kinetic energy and dissipation rate are

$$R\tilde{u}_i \frac{\partial K}{\partial x_i} = \frac{\partial}{\partial x_i}\left[\left(\frac{1}{R_T} + \frac{1}{R_\ell}\right)\frac{\partial K}{\partial x_i}\right] - R\widetilde{u_i'' u_j''}\frac{\partial \tilde{u}_i}{\partial x_j} - RE \quad (1)$$

$$R\tilde{u}_i \frac{\partial E}{\partial x_i} = \frac{\partial}{\partial x_i}\left[\left(\frac{1}{R_T \sigma_\epsilon} + \frac{1}{R_\ell}\right)\frac{\partial E}{\partial x_i}\right] - C_2 f_1 R \frac{E}{K}\widetilde{u_i'' u_j''}\frac{\partial \tilde{u}_i}{\partial x_j}, \quad - C_2 f_2 \frac{E^2}{K} \quad (2)$$

Equations (1) and (2) differ from the "ordinary" $k$-$\epsilon$ equations in several respects. First, functions $f_1$ and $f_2$ multiply the last two terms on the right side of Eq. (2). They are correction functions to 1) increase the production of dissipation near a wall as compared to the production rate ($f_1 \to 1$ far away from the wall) and 2) maintain a finite dissipation rate derivative at the wall, respectively. These functions are

$$f_1 = 1 + \left(A_{c\ell}/f_\mu\right)^3 \quad (3)$$

$$f_2 = 1 - e^{-R_t} \quad (4)$$

with $A_{c\ell} = 0.05$. The function $f_\mu$, appearing in Eq. (3), comes from the corrected law for turbulent viscosity, which is

$$\mu_T = C_\mu \rho f_\mu k^2/\epsilon \tag{5}$$

The function $f_\mu$ is given by

$$f_\mu = (1 - e^{-A_\mu R_k})^2[1 + (A_t/R_t)] \tag{6}$$

The behavior exhibited by $f_\mu$ is to go to unity away from the wall but to exhibit diminished value while retaining $y^4$ behavior near the wall. The values of $A_\mu$ and $A_t$ are 0.0165 and 20.5, respectively. In the Nomenclature, it should be noted that the Reynolds number $R_k$ contains a variable density and a stretched boundary-layer coordinate in place of the original constant density and $y$ of Ref. 6. The value of $C_\mu$ is taken as 0.09, in accordance with usual practice.

A second important deviation from the usual presentation of Eq. (2) lies in the constant $C_2$ in front of the second term on the right side of Eq. (2). More usually, this constant is designated $C_1$ and is less than $C_2$. It was found in Ref. 12 that unless the constants in front of the last two terms on the right side of Eq. (2) are the same, a singularity would occur in the approach inviscid flow to the stagnation point and no meaningful boundary condition on the viscous layer edge could be developed. The change made does not disturb the rate of decay of turbulence due to dissipation but increases the dissipation production rate. This is in accord with the observation in Ref. 16 that, in a decelerating flow, there is an increased production of dissipation due to the normal stresses. This was incorporated in an effective change of $C_1$ in Ref. 17 to account for this fact. The change made here is in the same direction, and the value taken for $C_2$ is 1.9, in accordance with usual practice. The remaining constant in Eq. (2), $\sigma_\epsilon$, is given its conventional value, 1.3.

### Stagnation-Point Problem

The remaining conservation equations of continuity, momentum, and energy are given in dimensional form as

$$\frac{\partial \rho}{\partial t} + \frac{\partial}{\partial x_i}(\rho U_i) = 0 \tag{7}$$

$$\rho\frac{\partial U_i}{\partial t} + \rho U_j \frac{\partial}{\partial x_j} U_i = -\frac{\partial P}{\partial x_i} + \frac{\partial}{\partial x_j}\tau_{ij} \tag{8}$$

$$\rho c_p\left(\frac{\partial T}{\partial t} + U_i \frac{\partial T}{\partial x_i}\right) = \frac{\partial}{\partial x_i}\left(\lambda \frac{\partial T}{\partial x_i}\right) \tag{9}$$

The procedure is then as follows:

1) Nondimensionalize the equations [Eqs. (7–9)].

2) Split all quantities into their Favre-average plus their Favre fluctuation except for the density, which is retained in its ordinary average and ordinary fluctuation form.

3) Time-average the equations.

4) Make certain modeling assumptions for turbulent momentum, heat, and density transport, which are given later.

5) Introduce the boundary-layer transformations.

$$v = V_2 R_\ell^{\frac{1}{2}}/V_\infty, \qquad y = x_2 R_\ell^{\frac{1}{2}}/c, \qquad x = x_1/c\eta = \int_0^y R\,\mathrm{d}y$$

$$\psi = \xi f(\eta), \qquad \xi = x, \qquad \tilde{u} = \xi f'$$

$$R\tilde{v} = -\frac{\partial \psi}{\partial \xi} - \frac{\partial \eta}{\partial x}\frac{\partial \Psi}{\partial \eta}$$

6) Choose dimensional pressure in the form

$$P_0 - \bar{p} = \frac{\rho_\infty V_\infty^2}{2c^2}\left[x^2 + F(y)\right] + \tfrac{2}{3}\bar{\rho}k$$

and if $c$ is chosen as related to the velocity gradient at infinity as

$$c = (-V_\infty)/(\mathrm{d}U_\infty/\mathrm{d}x)$$

this form of the pressure law will automatically satisfy the steady-state form of Eq. (8) at the edge of the viscous layer in the absence of turbulence. The addition of the turbulence term in the preceding equation arises naturally in this procedure and yields the direct observation that pressure and turbulence kinetic energy are mutually convertible. For a circular cylinder, it should be noted that $c = 2a$.

7) Seek solutions for which $u$ and shear stress are linear in $x$ and all other physical quantities are functions only of $\eta$. This is equivalent to seeking solutions in an $x$ power series from the nose and retaining only the first term.

8) Throw out terms that are of the order of $R_\ell^{-\frac{1}{2}}$ or $R_T^{-\frac{1}{2}}$ compared with unity.

The result is the following set of ordinary differential equations in the variable $\eta$ obtained from Eqs. (2), (3), (7–9):

$$f''' + \left(\frac{R_\ell}{R_T} R f''\right)' + ff'' + f'^2 - g = 0 \tag{10}$$

$$g'' + \left(\frac{P_r}{\sigma_T}\frac{R_\ell}{R_T} R g'\right)' + P_r f g' = -\overline{g}'' \tag{11}$$

$$K'' + \left(R\frac{R_\ell}{R_T}K'\right)' + \frac{P}{R} + fK' - E = 0 \tag{12}$$

$$E'' + \left(R\frac{R_\ell}{R_T}\frac{E'}{\sigma_\epsilon}\right)' + fE' + C_2\frac{E}{K}\left(f_1\frac{P}{R} - f_2 E\right) = 0$$

$$P = \left(\frac{RK}{g} - \frac{fg'}{R_T}\right)fg' + \frac{1}{R_T}(4f'^2 + g'f) \tag{13}$$

There have been several modeling assumptions in Eqs. (10–14). First, the relation between the stresses and the rate of strain is taken from Jones[16] as

$$\overline{\rho U_i'' U_j''} = 2/3\delta_{ij}\left(\bar{\rho}k + \mu_T\frac{\partial \tilde{U}_\ell}{\partial x_\ell}\right) - \mu_T\left(\frac{\partial \tilde{U}_i}{\partial x_j} + \frac{\partial \tilde{U}_j}{\partial x_i}\right)$$

Second, the quantity $\overline{u''} = -\overline{R'u'}$ is treated by gradient diffusion and is modeled as

$$\frac{1}{R_T}\frac{1}{\bar{\rho}}\frac{\partial \bar{\rho}}{\partial x}$$

Turbulent heat flux is also modeled by the gradient diffusion law

$$\overline{\rho V_i'' T''} = -\mu_T\frac{\partial \tilde{T}}{\partial x_i}$$

Third, with lack of justification, the Favre fluctuation in molecular viscosity $\mu''$ is neglected because there is no accepted model for it. The value of $\mu''$ will be small near a constant temperature wall and, near the outer edge of the viscous layer, turbulence effects dominate molecular effects, so the effect of molecular viscosity will be small. The hope is that the effect is small everywhere. Fourth, in the turbulent kinetic-energy equation, the velocity-pressure gradient correlation has been neglected. This issue will be returned to in future work. Finally, it will be seen that the static pressure has very little $\eta$ variation so that the perfect gas law has been used in the form

$$p = Rg = 1$$

Now, upon inspection of Eq. (11), it is seen that another unknown has appeared, which is

$$\overline{g''} = \overline{R(\rho g''^2/\rho)} \equiv Rq$$

The quantity $q$ may be calculated by a conservation equation derived for it. The procedure is to multiply the energy equation (9) by $g''$, split all quantities except density into their Favre mean and fluctuating quantities, and then time-average the equation, using the mean energy equation. Where diffusion terms arise, gradient diffusion is assumed, and a dissipation term is modeled in usual fashion. The result is

$$q'' + \left(\frac{P_r}{\sigma_T}\frac{R_\ell}{R_T}Rq'\right)' + P_r f q' - \frac{E}{K}q + 2\frac{P_r}{\sigma_T}\frac{R_\ell}{R_T}Rg'^2 - 2Rqg'' = 0 \tag{14}$$

where the fourth term represents the dissipation of the temperature fluctuations. It is seen that in Eq. (14), even if there is a point in the flowfield at which $q=0$, a $q$ will be generated by the production term if there is mean heat transfer ($g' \neq 0$).

The equation for the momentum conservation in the direction perpendicular to the wall (not shown) is really an equation for the static pressure and may be solved by quadrature after the rest of the field is determined. The form of the solution is that

$$(P_0 - p - 2/3kR)/\rho_\infty V_\infty^2 \text{ is } \mathcal{O}(1/R_\ell \text{ or } 1/R_T)$$

which shows that, as the turbulence decays toward the wall, some of the energy is converted to static pressure. The major conclusion, however, at least for moderate turbulence levels and high $R_T$, is that the static pressure is nearly constant in the direction normal to the wall, justifying the above treatment of the equation of state.

#### Boundary Conditions

The system of ordinary equations represented by Eqs. (10) and (12–14) represents an eleventh-order system, and eleven boundary conditions are required. Obvious conditions are

$$f(0) = 0 \text{ for an impermeable wall}$$
$$= f_0 \text{ specified for a given blowing rate} \tag{15}$$

$$f'(0) = 0 \tag{16}$$

$$f'(\infty) = 1 \tag{17}$$

$$g(0) = g_0 \text{ for a specified wall temperature} \tag{18}$$

$$g(\infty) = 1 \tag{19}$$

$$K(0) = q(0) = 0 \tag{20}$$

$$E(0) = E_0 \text{ which will be found to set the turbulence level} \tag{21}$$

From Ref. 13, a further condition at infinity is that production must equal dissipation so that

$$K(\infty)/E(\infty) = 1/\left(2C_\mu^{\frac{1}{2}}\right) \tag{22}$$

Since $K \propto \eta^2$ near the wall,

$$K'(0) = 0 \tag{23}$$

The final condition is that there be a convective-dissipation balance in the $q$ equation at infinity. Given the other conditions, this will occur if

$$q''(\infty) = 0 \tag{24}$$

This completes the specification of the boundary conditions. The problem is common in boundary-layer problems: the boundary conditions are applied in mixed fashion at either end of the calculation domain. Moreover, while in laminar problems the effective numerical position of infinity is usually known, in turbulence problems it is not clear where the effective value of infinity may be.

#### Numerical Problem

The senior author's experience with simpler stagnation-point flows indicated that there would probably be no particular problem in using a shooting method to solve this two-point boundary-condition problem. Consequently, such a method was chosen. However, in retrospect, other methods should have been investigated because of an extreme numerical sensitivity that arose in this turbulence problem. Discussion of this sensitivity follows.

The system of five nonlinear differential equations was split into a system of eleven first-order equations, and the equations were integrated outward from the wall using a fourth-order Runge-Kutta quadrature for simultaneous equations. The missing boundary conditions at the wall, $f''(0)$, $g'(0)$, and $E'(0)$, were guessed and then iterated by interval halving and the method of false position until the boundary conditions at infinity were satisfied. The question of what value of $\eta$ to ascribe to infinity depended on the Reynolds number of the run. Since the turbulence significantly thickens the viscous layer over its laminar counterpart, usual values for a laminar calculation, say, $\eta = 6$, were not sufficient. The higher the laminar Reynolds number, the thinner the molecular viscous region compared to the overall turbulent layer. In the dimensionless distance variable, this meant that the higher the laminar Reynolds number, the larger $\eta$ had to be in order to reach infinity. Values of 10–30 were used, depending on $R_\ell$.

The actual start of the integration at the wall presents a slight problem because the $K$, $E$, and $q$ equations are singular at the wall, containing terms like 0/0. To start the integration, power series of the form

$$K = K_2\eta^2 + \ldots, \qquad E = E_0 + E_1\eta + \ldots, \qquad q = Q_2\eta^2 + \ldots$$

are chosen. The quantity $E_1$ is the unknown boundary condition $E'(0)$. From Eq. (12), it may be deduced that dissipation and diffusion are in balance at the wall, and consequently $2K_2 = E_0$. The chosen value for $E_0$ actually specifies the value of the turbulence level at the edge of the viscous layer. The above power series are used for a single step away from the wall, and then a full integration takes place.

A calculation shown in Fig. 2 illustrates the extreme numerical sensitivity to choice of initial conditions. The calculation is for a constant-density flow, and the sensitivity of the turbulent kinetic energy to the choice of the initial $E'(0)$ is shown. Only an extremely narrow range of this parameter will allow a solution at all, and differences in the third significant figure give the differences between exponentially growing or decaying solutions. The numerical problem, therefore, consists of first finding a very narrow range of $E'(0)$ in which to search for solutions and then carrying out the iterations while dealing in the last few significant digits of this quantity.

In the calculations below, consisting of either constant density or weak heat-transfer results, the $q$ equation plays no role. It will play a role in a strong heat-transfer case. However, it is an equation more or less "carried along for the ride," since as long as Eqs. (15–23) are satisfied, Eq. (24) will also be satisfied. That is, any choice of $Q_2$ will yield a satisfactory solution to the $q$ equation. The choice of $Q_2$ merely sets the value of the edge value of the temperature fluctuations coming from the freestream. In the present work, this will be zero.

### Matching with the Freestream

In the outer inviscid flow, the velocity normal to the body (in this case, a cylinder) on the stagnation streamline behaves as shown in Fig. 3. Very near the body, the slope of this velocity is $-2a$. This value was used in Ref. 12 to construct an exact solution to the inviscid stagnation process for the turbulence and create a link between the freestream turbulence quantities and those at the edge of the viscous layer. However, an interpretation problem arises in that solution because of the assumed slope of $-2a$, where it is obvious that the slope varies from 0 to $-2a$ during the entire stagnation process. The analytical condition between the boundary-layer edge conditions and the freestream turbulence conditions is given as

$$K_s/K_0 = \left(2\gamma C_\mu V_\infty k_0/a\epsilon_0\right)^{(1/C_2-1)} \tag{25}$$

It appears that if this solution is to be used, some kind of average value of $\gamma$ should be taken, modeling the stagnation process as an effective linear decay of velocity from the freestream velocity at infinity to zero and defining infinity as the point where the freestream velocity is encountered in the straight-line approximation. This kind of approximation was also used in Ref. 4. In any event, this slope appears as an adjustable constant in the theory to best match experiment. It should be noted that this is the *only* adjustable constant in the theory presented. For the best match of theory and experiment, the constant $\gamma = -0.8$ has been chosen.

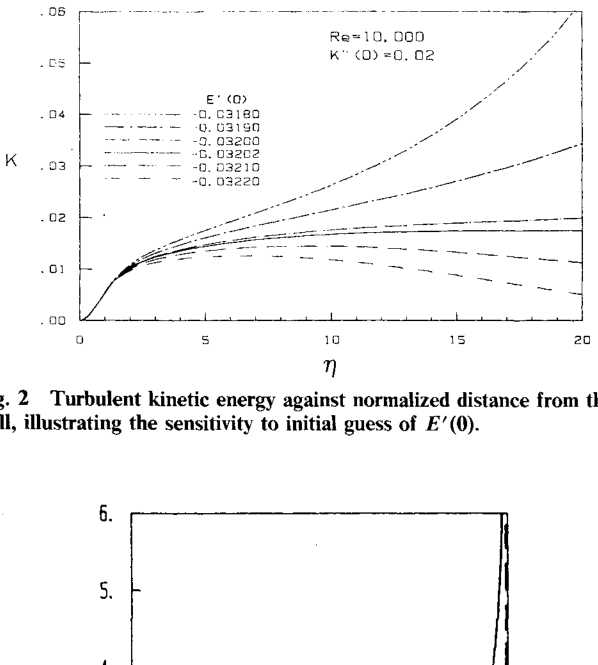


**Fig. 2 Turbulent kinetic energy against normalized distance from the wall, illustrating the sensitivity to initial guess of $E'(0)$.**

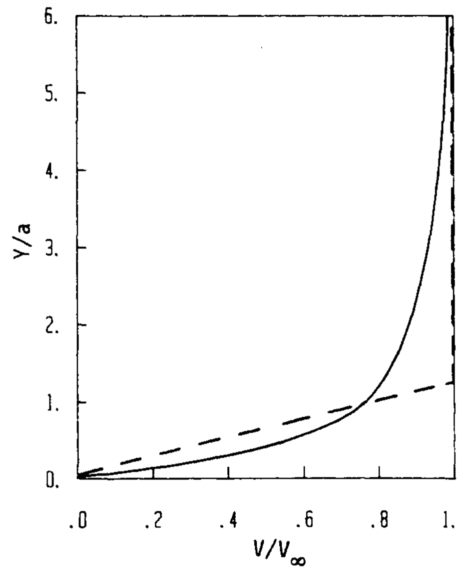


**Fig. 3 Inviscid stagnation-point flow, showing the decay of the velocity perpendicular to the wall and the straight-line approximation used here to calculate the effective freestream turbulence properties.**

## Results

### Constant Density

Typical velocity (parallel to the wall) distribution functions are shown in Fig. 4 for laminar and turbulent flow. Evident are a large thickening of the viscous zone due to the turbulence and, at the same time, a steepening of the gradient near the wall. The effect is shown here for a large laminar Reynolds number, because the effect is larger when the Reynolds number is larger. The reason for this is that, the larger the Reynolds number, the thinner the laminar viscous zone, and the turbulence is therefore better able to penetrate the viscous layer toward the wall. Figure 4 illustrates the problem mentioned earlier that large values of $\eta$ are required, compared to the laminar problem, for the quantities such as $f'$ to approach their viscous edge conditions. The analytical reason for this is that the viscous distance scale near the outer edge is dominated by the turbulent Reynolds number, whereas the distances have been scaled by the laminar Reynolds number in order to behave most properly near the wall.

In Fig. 5, $f''(0)$ is shown proportional to the shear stress at the wall. The velocity gradient steepening effect clearly depends strongly on the Reynolds number. Recall that $K''(0)$ is related to the general turbulence level in the layer. The relationship, shown in Fig. 6, is not linear but monotonic.

The distribution of the various sources and sinks in the turbulent kinetic-energy equation is shown in Fig. 7. The domination of diffusion and dissipation near the wall gives way to a balance between production and dissipation near the outer edge, as a boundary condition demands. One other region of interest is near the wall where there is a narrow region of convection-dissipation balance.

While the constant-density case is interesting for some physical effects, it is not amenable to experimental test. For example, the shear stress is zero and nonmeasurable at the stagnation point. Consequently, one must move to the heat-transfer case for experimental test of the method.

### Variable Density

In the case of heat transfer near a stagnation point, the heat transfer is given by

$$q_w = h(T_w - T_\infty)$$

where the heat-transfer coefficient is given in dimensionless form through the Nusselt number. Tracing through the transformations,

$$Nu_D/Re_D = -2g'(0)/(g(0)-1)$$

where quantities have been defined as positive for a case where the wall is heating the surroundings. One of the more extensive sets of data for stagnation-point heat transfer is that due to Smith and Kuethe;[4] these data will be used for comparison to the present theory. The work corresponds to a case of very weak overheat of a circular cylinder. The weak overheat means that, for all practical purposes, the density is nearly constant, so that these data will not really test the complete variable-density formulation of the theory. However, a test will be given to the Lam-Bremhorst formulation and to the method of handling the viscous-layer/freestream transition. All heat-transfer calculations have been made with $p_r = 0.71$, with a turbulent Prandtl number of 0.9.

The chosen data do not contain measurements of both intensity and scale of the approach turbulence, but the current

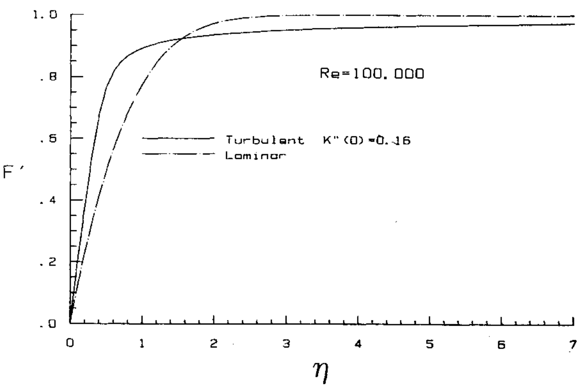


Fig. 4 Velocity parallel to the wall in laminar and turbulent flow.

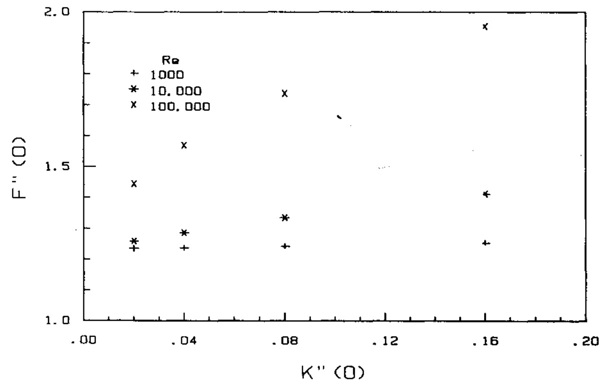


Fig. 5 Wall shear stress as a function of the turbulent kinetic-energy curvature at the wall.

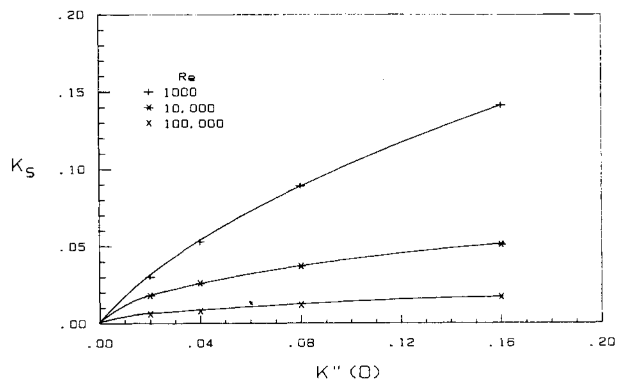


Fig. 6 Relation between the turbulent kinetic-energy curvature at the wall to the turbulent kinetic-energy at the edge of the viscous zone.

theory uses both. In order to estimate the length-scale properties of the turbulence of Ref. 2, it is noted that the turbulence-generating grid is quite close in geometric design to one for which length-scale data are presented in Ref. 18. A curve fit to the length-scale data reveals that

$$L_f/M = 0.348 + 0.00754(x/M) - 2.98{*}10^{-5}(x/M)^2$$

and the mesh $M$ was 1 in. This is used to calculate the length-scale information at various distances from the grid as

$$u'_\infty = 0.0127 + 4.88x^{1.8} \; (x \text{ in in.})$$

which was also used in the data-comparison procedure. Assuming isotropic turbulence at the edge of the viscous layer (which is almost certainly not true), the relation between

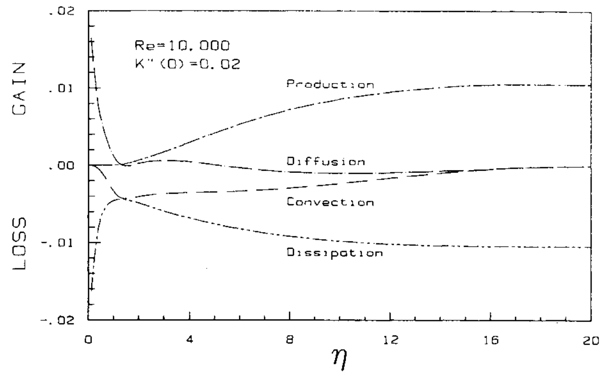


Fig. 7 Turbulent kinetic-energy budget.

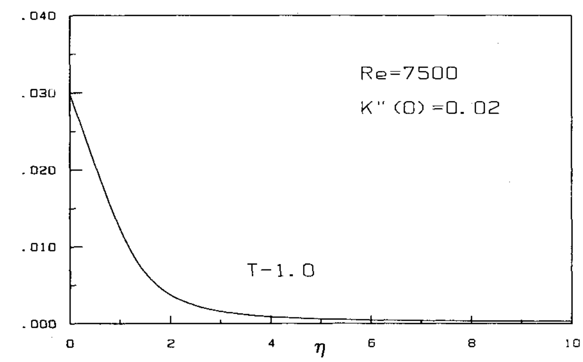


Fig. 8 Temperature profile in a typical case with a hot wall.

turbulence kinetic energy and $u'_\infty$ is

$$K_0 = 1.5{*}u'^2_\infty$$

The temperature profile for a typical calculation is shown in Fig. 8 with the weak overheat of Ref. 2. Seen again is a rapid transition in the molecular near-wall mixing layer, but with a rather long falloff to the boundary condition at the viscous-layer edge.

Comparison of theory and experiment is shown in Fig. 9, using a plot format taken directly from Ref. 2 and the data points located thereon. The solid points are calculated points, and the open data points are distinguished as one or the other of two kinds, depending on the cylinder diameter used in the experiments. The experiments were run by varying the tunnel speed and distance of the cylinder from the turbulence grid. It is important to notice that there was only one Reynolds number at which cylinders of both diameters were tested. In Ref. 2, the value of $u'_\infty$ was selected as the value that occurred downstream of the grid in undisturbed flow at the location of the stagnation point in the calculation to account for the deceleration in the inviscid portion of the stagnation process.

The following points are to be noted in Fig. 9:

1) As the turbulence intensity rises, the heat transfer rises both theoretically and experimentally, as is to be expected.

2) As the Reynolds number rises, the heat transfer rises both theoretically and experimentally. This is to be expected because of the thinner, molecular-dominated mixing layer and greater penetration of the turbulence toward the wall.

3) At the higher Reynolds numbers, there is on-average agreement with experiment, but the heat transfer is overpredicted by the model for the 8-in. diam cylinder, which was the only one tested at the highest Reynolds number. The difference between the theoretical results for the 3- and 8-in. diam cylinders can be traced directly to the model used for the deceleration process external to the viscous zone. This is an

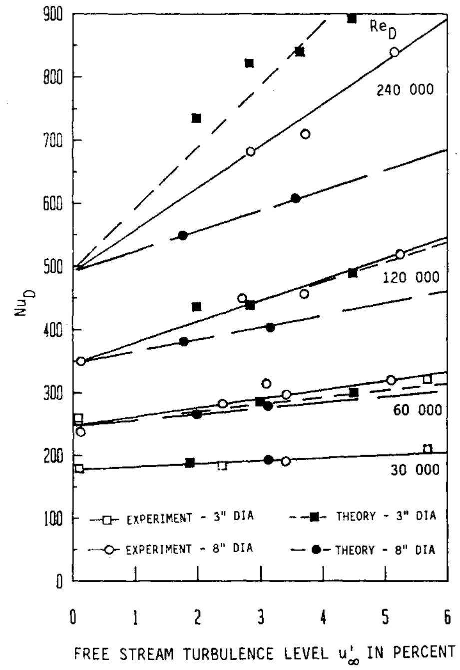


**Fig. 9 Comparison of theory and experiment (data from Ref. 2).**

effect of the ratio of turbulence to physical length scales in the theory.

4) Straight lines are plotted in Fig. 9 because they appeared in the plot of Ref. 2. However, theory indicates some curvature, which would actually be expected, since the theory and physical reasoning would not suggest a linear heat-transfer rate in the turbulence intensity. That is, no dimensional analysis, with the turbulence model used here, would pull out a linear relationship between the Nusselt number and the intensity.

Not shown on Fig. 9 are the theoretical curves that would be obtained if it had been assumed that there was no effect of the external deceleration process. As may be expected, since the deceleration process creates turbulence, the heat transfer would be underpredicted. This indicates that the process considered is important, but it is not accurately treated here. Moreover, there is a need for experimentation in this area to gain a quantitative hold on the external deceleration process. In particular, there is a need for experimentation at high Reynolds number with independent variation of diameter, turbulence length scale, turbulence intensity, and Reynolds number with varying overheat and/or underheat.

## Concluding Remarks

An extension of the Lam-Bremhorst turbulence model has been made for variable-density flows and has been applied to heat-transfer calculations for a two-dimensional, planar flow over cylinders. This model 1) corrects past deficiencies in treatment of the proper behavior of the turbulence near the wall, 2) introduces no new empirical constants, 3) presents a new formulation to account for variable density and temperature fluctuations in the approach stream, and 4) appears to work well for the viscous (molecular and turbulent) layer adjacent to the wall. Application of the method requires, however, that account be given to the inviscid deceleration process external to the viscous zone, and it appears that this part of the theory is somewhat deficient, especially at the higher Reynolds numbers against which the theory was tested.

There appear to be several needs. First, the inviscid deceleration process needs to be revisited through perhaps a stress transport model or with a dissipation equation such as that used in Ref. 17 or with a numerical integration of the deceleration process rather than the approximate method used here. Second, experiments are needed on this deceleration process with independent variation of Reynolds number, turbulence to physical length-scale ratio, relative turbulence intensity and over- or underheat. Third, since the calculations have not really pressed the variable density and the fluctuating temperature problem, calculations for the high-heat-transfer case need to be made. However, the authors know of no experiments against which to compare the calculations; experimentation is needed in this area.

## Acknowledgments

This work was supported by the U.S. Army Office of Research under Contract DAAG29-83-K-0143.

## References


[1] Galloway, T.R., "Enhancement of Stagnation Flow Heat and Mass Transfer through Interactions of Free Stream Turbulence," *American Institute of Chemical Engineering Journal*, Vol. 19, May 1973, pp. 608–617.

[2] Smith, M.C. and Kuethe, A.M., "Effects of Turbulence on Laminar Skin Friction and Heat Transfer," *Physics of Fluids*, Vol. 9, Dec. 1966, pp. 2337–2344.

[3] Gorla, S.R., "Effects of Unsteady Free Stream Velocity and Free Stream Turbulence on Stagnation Point Heat Transfer," NASA CR-3804, June 1984.

[4] Traci, R.M. and Wilcox, D.C., "Freestream Turbulence Effects on Stagnation Point Heat Transfer," *AIAA Journal*, Vol. 13, July 1975, pp. 890–896.

[5] Fairweather, M., Kilham, J.K., and Mohebi-Ashtiani, A., "Stagnation Point Heat Transfer from Turbulent Methane-Air Flames," *Combustion Science and Technology*, Vol. 35, 1984, pp. 225–238.

[6] Lam, C.K.G. and Bremhorst, K., "A Modified Form of the $k$-$\epsilon$ Model for Predicting Wall Turbulence," *Journal for Fluids Engineering*, Vol. 103, Sept. 1981, pp. 456–460.

[7] Jones, W.P. and Launder, B.E., "The Prediction of Laminarization with a Two-Equation Model of Turbulence," *International Journal of Heat and Mass Transfer*, Vol. 15, 1972, pp. 301–312.

[8] Jones, W.P. and Launder, B.E., "Calculation of Low Reynolds Number Phenomena with a Two-Equation Model of Turbulence," *International Journal of Heat and Mass Transfer*, Vol. 16, 1973, pp. 1119–1130.

[9] Hoffman, G.H., "Improved Form of the Low Reynolds Number $k$-$\epsilon$ Model," *Physics of Fluids*, Vol. 18, March 1975, pp. 309–312.

[10] Chien, J.C., "Numerical Analysis of Turbulent Separated Subsonic Diffuser Flow," *Symposium on Turbulent Shear Flows*, Vol. 1, 1977, pp. 18.19–18.25.

[11] Hassid, S. and Poreh, M., "A Turbulent Energy Dissipation Model for Flows with Drag Reduction," *Journal of Fluids Engineering*, Vol. 100, March 1978, pp. 107–112.

[12] Strahle, W.C., "Stagnation Point Flows with Freestream Turbulence—The Matching Condition," *AIAA Journal*, Vol. 23, Nov. 1985, pp. 1822–1823.

[13] Bearman, P.W., "Some Measurements of the Distortion of Turbulence Approaching a Two-Dimensional Bluff Body," *Journal of Fluid Mechanics*, Vol. 53, Pt. 3, 1972.

[14] Sadeh, W.Z., Sutera, S.P., and Maeder, P.F., "An Investigation of Vorticity Amplification in Stagnation Point Flow," *Zeitschrift fuer Angewandte Mathematik und Physik*, Vol. 21, 1970, pp. 699–716.

[15] Jones, W.P., "Models for Turbulent Flows with Variable Density and Combustion," *Predictive Methods for Turbulent Flows*, edited by W. Kollman, Hemisphere, New York, 1980, pp. 379–422.

[16] Hanjalic, K. and Launder, B.E., "Preferential Spectral Transport by Irrotational Straining," *Turbulent Boundary Layers*, ASME, New York, 1979, pp. 101–110.

[17] Leschziner, M.A. and Rodi, W., "Calculation of Annular and Twin Parallel Jets Using Various Discretization Schemes and Turbulence-Model Variations," *Journal of Fluids Engineering*, Vol. 103, June 1981, pp. 352–360.

[18] Raithby, G.D. and Eckert, E.R.G., "The Effect of Turbulence Parameters and Support Position on the Heat Transfer from Spheres," *International Journal of Heat and Mass Transfer*, Vol. 11, 1968, pp. 1233–1252.